

ANALOG ERROR CORRECTION VIA TUBE PACKING

Robert M. Taylor Jr., Lamine Mili, Amir I. Zaghloul

Bradley Department of Electrical Engineering
Northern Virginia Center, Virginia Tech
Falls Church, VA 22043

ABSTRACT

Analog error correction in the form of bandwidth expansion Shannon-Kotelnikov maps allow us to directly map a given source symbol to multiple channel inputs thereby combining source and channel coding into a single vector-valued mapping function. These joint source-channel codes have the potential to approach Shannon's optimal performance theoretically achievable (OPTA) with minimal delay and complexity, but currently there are no theoretical constructions for how to find them. This is particularly the case for dimensions greater than two. This paper proposes a framework for analog coding based on densely packing (hyper)tubes inside of (hyper)spheres whereby the center line of the hypertube is a bounded 1-D manifold corresponding to the image of our desired encoder map. We show for dimensions two, three, and four that this construction method provides extremely simple yet powerful source-channel codes that roughly follow the slope of the OPTA curve in the low SNR region. The tube packing density decreases with increasing dimension which may explain the increasing gap to OPTA as the dimension grows.

Index Terms— Shannon-Kotelnikov, analog error correction, tube packing

1. INTRODUCTION

Joint source-channel codes (JSCC) are formed by merging the source and channel coder into a single map such that the source symbol is mapped directly to the channel input. These direct maps, which are also known as Shannon-Kotelnikov (SK) maps [1, 2], have the potential to achieve Shannon's optimal performance theoretically achievable (OPTA) with single-letter codes in the memoryless case or minimal delay otherwise [3]. When the source bandwidth is smaller than the allowable channel bandwidth, we may create bandwidth expansion maps whereby one source symbol can be mapped to multiple channel input symbols allowing for error correction. In this study we focus attention on bandwidth expansion maps applied to continuous-valued source symbols and thereby consider our SK map as an analog error correction scheme.

Previous work on bandwidth expansion SK maps including theory and application can be found in such works as [4, 5, 6] and references therein. Nearly all the works describe variations on a 2-D Archimedes spiral, but no general theory is laid out for higher dimensional expansions. A 1:3 bandwidth expansion approach is given [7] which combines a scalar quantizer with a 2-D Archimedes spiral, but the gap to OPTA is quite large. Furthermore, nearly all research in this area has focused on Gaussian sources, whereas we consider uniformly distributed sources in this work.

Kravtsov et al. [8] were the first to present the beginning of a theoretical framework for higher dimensional SK maps. They proved that 1: n analog codes formed by densely packing tubes inside a hypersphere led to performance gains of n dB source-to-distortion ratio for each 1 dB of channel signal-to-noise ratio (SNR) for uniformly distributed sources in an additive white Gaussian noise (AWGN) channels in the high SNR region. This performance slope follows the slope of OPTA curves and is therefore worthy of consideration. Ziv [9] showed that optimal bandwidth expansion encoding maps vary as a function of SNR and therefore code selection will be a function of the target channel signal to noise ratio (SNR). In this work, we build on the tube packing concepts presented in [8] and bring in basic concepts from differential geometry of "thick" curves (or tubes) to design 1: n analog codes for dimensions $n = 2, 3, 4$ that follow the slope of the OPTA curve in the low SNR region and leave relatively small gaps to OPTA.

The rest of this paper is organized as follows. In Section 2 we give brief mathematical preliminaries on differential geometry of curves and tubes and define OPTA. In Section 3 we describe our method of code construction based on designing "thick" curves of constant generalized curvature and give simulation performance results in Section 4.

2. MATHEMATICAL PRELIMINARIES

2.1. Differential geometry of curves

A curve \mathbf{x} is a vector-valued bijective function that maps an interval I of the real line to a 1-D manifold \mathcal{M}_1 embedded in

R. M. Taylor Jr. is also with MITRE Corporation McLean, VA 22102.

n -dimensional Euclidean space such that

$$\mathbf{x} : I \rightarrow \mathcal{M}_1 \subset \mathbb{R}^n \quad (1)$$

where \mathbf{x} is called a parametric curve of class C^r if \mathbf{x} is r times continuously differentiable. The curve \mathbf{x} is parameterized by $\alpha \in I$ and $\mathbf{x}(I)$ is the image of the curve. A C^r curve is regular of order m if for any $\alpha \in I$, $\{\mathbf{x}'(\alpha), \mathbf{x}''(\alpha), \dots, \mathbf{x}^{(m)}(\alpha)\}$, $m \leq k$ are linearly independent vectors in \mathbb{R}^n . We can define the Frenet frame for the curve \mathbf{x} as the set of orthonormal vectors $\mathbf{e}_1(\alpha), \dots, \mathbf{e}_n(\alpha)$ formed as

$$\begin{aligned} \mathbf{e}_1(\alpha) &= \mathbf{x}'(\alpha) / \|\mathbf{x}'(\alpha)\|, \quad \mathbf{e}_j(\alpha) = \frac{\tilde{\mathbf{e}}_j(\alpha)}{\|\tilde{\mathbf{e}}_j(\alpha)\|} \\ \tilde{\mathbf{e}}_j(\alpha) &= \mathbf{x}^{(j)}(\alpha) - \sum_{i=1}^{j-1} \langle \mathbf{x}^{(j)}(\alpha), \mathbf{e}_i(\alpha) \rangle \mathbf{e}_i(\alpha) \end{aligned} \quad (2)$$

from Gram-Schmidt orthogonalization. The generalized curvatures are the $n - 1$ real-valued functions $\chi_i(\alpha)$ formed as

$$\chi_i(\alpha) = \frac{\langle \mathbf{e}'_i(\alpha), \mathbf{e}_{i+1}(\alpha) \rangle}{\|\mathbf{x}(\alpha)\|} \quad i = 1, 2, \dots, n - 1 \quad (3)$$

where $\langle \cdot, \cdot \rangle$ denotes inner product both in (2) and (3) and $\|\cdot\|$ is the L_2 -norm. From (3) we can write a system of first order differential equations known as the Frenet-Serret formula

$$[\mathbf{e}'_1(\alpha), \dots, \mathbf{e}'_n(\alpha)]^T = \|\mathbf{x}'(\alpha)\| \mathbf{B} [\mathbf{e}_1(\alpha), \dots, \mathbf{e}_n(\alpha)]^T \quad (4)$$

where \mathbf{B} is a skew-symmetric matrix composed of the generalized curvatures

$$\mathbf{B} = \begin{bmatrix} 0 & \chi_1(\alpha) & \cdots & 0 & 0 \\ -\chi_1(\alpha) & 0 & \cdots & 0 & 0 \\ \vdots & \vdots & \ddots & \vdots & \vdots \\ 0 & 0 & \cdots & 0 & \chi_{n-1}(\alpha) \\ 0 & 0 & \cdots & -\chi_{n-1}(\alpha) & 0 \end{bmatrix}. \quad (5)$$

The fundamental theorem of curves states that given n parametric functions $\chi_i \in C^{n-i}([a, b])$, $1 \leq i \leq n$ with $\chi_i(\alpha) > 0, \forall i$, there exists a regular C^{n+1} curve \mathbf{x} which is unique up to transformations under the Euclidean group. This means we can translate, rotate, or scale the image of the curve (thereby modifying the parameters of the map accordingly), and it will not change the generalized curvatures. This will be a useful property later in section 3.2 when we seek to optimize the parameters of our encoder functions.

2.2. Global radius of curvature

The theory of curves above is not enough to establish our method of tube packing since there is no inherent thickness property of 1-D manifolds. We desire a mathematical tool that will convey the idea of insulation and prevent our tubes from self intersecting or bending too tightly. The global radius of curvature introduced in [10] (in the context of knot

theory) is one such way to ascribe an insulating radius about the center line of a curve. The circumradius function of a curve using tangent-point form can be written as:

$$\rho(\alpha_1, \alpha_2) = \frac{\|\mathbf{x}(\alpha_1) - \mathbf{x}(\alpha_2)\|}{2|\sin \angle(\mathbf{x}(\alpha_1) - \mathbf{x}(\alpha_2), \mathbf{x}'(\alpha_2))|} \quad (6)$$

where $\angle(\cdot, \cdot)$ denotes the angle between two vectors, α_i are different arc-length parameter instances corresponding to distinct points on the curve. Squaring this function and eliminating the sine term we can write $\rho^2(\alpha_1, \alpha_2)$ as

$$\frac{\frac{1}{4} \|\mathbf{x}(\alpha_1) - \mathbf{x}(\alpha_2)\|^4 \|\mathbf{x}'(\alpha_2)\|^2}{\|\mathbf{x}(\alpha_1) - \mathbf{x}(\alpha_2)\|^2 \|\mathbf{x}'(\alpha_2)\|^2 - |\langle \mathbf{x}(\alpha_1) - \mathbf{x}(\alpha_2), \mathbf{x}'(\alpha_2) \rangle|^2} \quad (7)$$

which is the form we will use in section 3. The local curvature (first generalized curvature) can be obtained directly from (3) or as reciprocal of the limiting case of the circumradius function as α_1 approaches α_2 . The global radius of curvature which defines our tube radius is then simply

$$\rho_g = \min_{\alpha_1, \alpha_2 \in I} \rho(\alpha_1, \alpha_2) \quad (8)$$

2.3. Optimal Performance Theoretically Achievable

In order to evaluate the performance of our analog coding scheme we must use OPTA to relate the source reconstruction distortion D to the input channel power P as:

$$R(D) = nC(P) \quad (9)$$

where $C(P)$ is the capacity cost function [3] and $R(D)$ is the rate-distortion function [11]. For AWGN channel with noise variance σ_w^2 and average power P we have $C(P) = \ln(1 + P/\sigma_w^2)/2$. Since there is no closed-form expression for $R(D)$ given a uniform source with mean square error distortion, we chose to approximate $R(D)$ with the Shannon lower bound [12]

$$R(D) \geq h(s) - \frac{1}{2} \ln(2\pi eD) \quad (10)$$

where $h(s)$ is the entropy of the source s , which for $s \sim U[0, 1]$ yields a source variance $\sigma_s^2 = 1/3$ and an entropy $h(s) = 0$. See e.g. [11] for entropies of various source distributions. Therefore, (10) reduces to $R(D) \geq -\ln(2\pi eD)/2$ and the OPTA in (9) for our formulation reduces to the relationship:

$$D \geq \frac{1}{2\pi e} \left(1 + \frac{P}{\sigma_w^2}\right)^{-n} \quad (11)$$

3. ANALOG CODE CONSTRUCTION

In Fig. 1 we illustrate the three basic components of Shannon-Kotelnikov source-channel coding: 1) encoder, 2) channel, and 3) decoder. In our problem formulation we consider only AWGN channels such that $\mathbf{y} = \mathbf{x} + \mathbf{w}$ where $\mathbf{w} \sim \mathcal{N}(0, \sigma_w^2 I)$

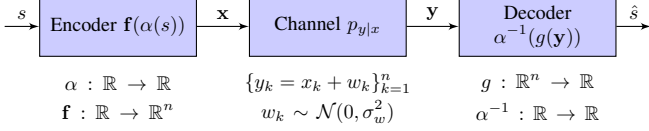


Fig. 1: Block diagram of Shannon-Kotelnikov joint source-channel coding architecture. A source s is encoded to \mathbf{x} , passed through a channel to create \mathbf{y} , and decoded to recover source estimate \hat{s} .

and only uniformly distributed sources $s \sim U[0, 1]$. The encoder is a curve as defined in section 2.1. In our formulation it is composed of a scalar-valued *stretching* function $\alpha(s)$ with a vector-valued *folding* function \mathbf{f} that together maps continuous source symbol s into channel input \mathbf{x} as $\mathbf{f} : \alpha(s) \mapsto \mathbf{x}$. The decoder is a surjective map composed of an *unfold* function g containing a vector input with an *unstretching* function $\alpha^{-1}(\cdot)$ that together maps channel output \mathbf{y} into source estimate $\hat{\alpha}$ as $g : \mathbf{y} \mapsto \hat{\alpha}$. We let $\alpha = Ls$ (constant uniform stretching) so that $\hat{s} = \hat{\alpha}/L$.

3.1. Constant Curvature Curves

We restrict our attention in this paper to encoder curves that have constant generalized curvature which means the terms χ_i for $i = 1, 2, \dots, n-1$ in (3) and (5) are constants to be determined. We can then generate the functional form of our encoder maps \mathbf{x} by solving the Frenet-Serret system of differential equations in (4). The resulting curves, circumradius functions, and first generalized curvatures as a function of the unknown parameters for $n = 2, 3, 4$ dimensions are given in Table 1 where we make the assignments

$$\begin{aligned} t_1 &= b^2 \Delta^2 + 2r^2(1 - \cos \Delta) \\ t_2 &= b^2 \Delta + r^2 \sin \Delta \\ t_3 &= r_1^2 + r_2^2 - r_1^2 \cos(\omega_1 \Delta) - r_2^2 \cos(\omega_2 \Delta) \\ t_4 &= r_1^2 \omega_1 \sin(\omega_1 \Delta) + r_2^2 \omega_2 \sin(\omega_2 \Delta) \end{aligned} \quad (12)$$

The circumradius function in the constant curvature case is only a function of the difference between the two arc-length instances which allows us to parameterize $\rho(\alpha_1, \alpha_2)$ as simply $\rho(\Delta)$ where $\Delta = \alpha_1 - \alpha_2$. From L'Hopital's rule we can verify that the circumradius function collapses back to the inverse local radius of curvature function χ_1^{-1} from (3) such that $\lim_{\Delta \rightarrow 0} \rho(\Delta) = \chi_1^{-1}$.

The 2-D curve is parameterized by r , the 3-D curve by r and b , and the 4-D curve by r_1, r_2, ω_1 , and ω_2 which are to be determined in section 3.2. There will only be two degrees of freedom for the 4-D case since it can be shown (as in [13]) that $r_1^2 \omega_1^2 + r_2^2 \omega_2^2 = 1$ and that the constant curvature curve lies on a 3-sphere. Thus, without loss of generality we set $r_1^2 + r_2^2 = 1$ which means $r_1 \in (0, 1)$. Furthermore, we have

\mathbf{x}	$\rho^2(\Delta)$	χ_1
$\begin{bmatrix} r \cos \alpha \\ r \sin \alpha \end{bmatrix}$	r^2	$\frac{1}{r}$
$\begin{bmatrix} r \cos \alpha \\ r \sin \alpha \\ b\alpha \end{bmatrix}$	$\frac{\frac{1}{4}t_1^2(b^2 + r^2)}{t_1(b^2 + r^2) - t_2^2}$	$\frac{r}{r^2 + b^2}$
$\begin{bmatrix} r_1 \cos(\omega_1 \alpha) \\ r_1 \sin(\omega_1 \alpha) \\ r_2 \cos(\omega_2 \alpha) \\ r_2 \sin(\omega_2 \alpha) \end{bmatrix}$	$\frac{t_3^2}{2t_3 - t_4^2}$	$\sqrt{r_1^2 \omega_1^4 + r_2^2 \omega_2^4}$

Table 1: Encoder map \mathbf{x} , squared circumradius function $\rho^2(\Delta)$, and first generalized curvature χ_1 for $n = 2$ (first row), $n = 3$ (second row), and $n = 4$ (third row) dimensional analog codes.

$\omega_2 = \sqrt{(1 - r_1^2 \omega_1^2)/(1 - r_1^2)}$ which means $\omega_1 \in (1, 1/r_1)$. Each of these curves also contains an additional path length parameter L such that $\alpha = Ls$ where $s \in [0, 1]$ causing L to act as a constant stretch factor [8].

The maximum likelihood (ML) decoder for the encoder maps given in Table 1 is given by $\hat{\alpha} = \underset{\alpha}{\operatorname{argmin}} \mathcal{D}_n^2(\alpha)$ where the squared distance \mathcal{D}_n^2 for $n = 2, 3, 4$ between the observed point and the closest point on the curve is given by

$$\begin{aligned} \mathcal{D}_2^2(\alpha) &= r^2 + \|\mathbf{y}\|^2 - 2r(y_1 \cos(\alpha) + y_2 \sin(\alpha)) \\ \mathcal{D}_3^2(\alpha) &= r^2 + \|\mathbf{y}\|^2 + \alpha^2 b^2 - 2by_3\alpha \\ &\quad - 2r(y_1 \cos(\alpha) + y_2 \sin(\alpha)) \\ \mathcal{D}_4^2(\alpha) &= r_1^2 + r_2^2 + \|\mathbf{y}\|^2 - 2r_1(y_1 \cos(\omega_1 \alpha) + \\ &\quad y_2 \sin(\omega_1 \alpha)) - 2r_2(y_3 \cos(\omega_2 \alpha) + y_4 \sin(\omega_2 \alpha)) \end{aligned} \quad (13)$$

for each of the three encoder maps tabulated in Table 1. Although the decoder functions are not closed form for these cases, accurate closed-form approximations can be found. For example, we can approximate the decoder for the 3-D case as

$$\hat{\alpha} = \left\lfloor \frac{y_3/b - \phi + \pi}{2\pi} \right\rfloor 2\pi + \phi \quad (14)$$

where $\phi = \operatorname{mod}(\operatorname{atan2}(y_2, y_1), 2\pi)$ and $\lfloor \cdot \rfloor$ denotes the floor operator.

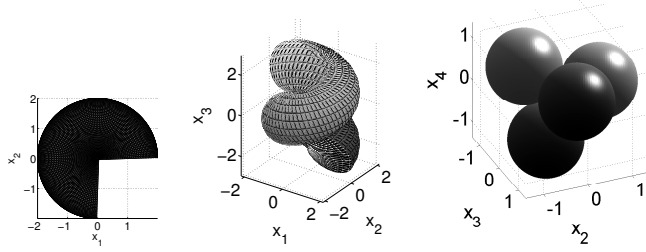
3.2. Optimization criteria for encoder parameters

Based on the results of [8] we know that packing density plays a key role in the performance of analog codes. We select the parameters of our encoder functions to maximize the density of the (hyper)-tube contained within the n -sphere such that the packing density d is defined as

$$d = \frac{\text{path length} \times (\text{tube cross-sectional volume})}{\text{Volume of bounding } n\text{-sphere}} \quad (15)$$

n	optimized parameters	density
2	$L = \sqrt{2\pi}, r = 1, \rho_g = 1$	0.707
3	$L = 3\pi, r = 1, b = .4, \rho_g = 1.16$	0.476
4	$L = 7.68, r_1 = 0.6, \omega_1 = 1.39, \rho_g = .8$	0.397

Table 2: Optimized parameters for curves in Table 1 by maximizing tube densities. It was noted in [15, 16] that the densest 3-D tube packing corresponded to $b = .4$ which matches our result.



(a) 2-D ribbon (b) 3-D tube (c) 4-D tube cross-section

Fig. 2: Dense tube packings computed from encoder maps in Table 1 with optimized parameters shown in Table 2.

where the total path length is:

$$\int_{\alpha=0}^L \|\mathbf{x}'(\alpha)\| d\alpha = L\|\mathbf{x}'(\alpha)\| \quad (16)$$

since the constant curvature assumption makes $\|\mathbf{x}'(\alpha)\|$ constant. Since the volume of a $(n-1)$ sphere is $V_n(R) = \mathcal{C}_n R^n$ where $\mathcal{C}_n = \pi^{n/2}/\Gamma(n/2 + 1)$ and $\Gamma(z) = \int_0^\infty e^{-t} t^{z-1} dt$ [14], the packing densities for the three cases in Table 1 can be written as $d_2 = 2Lr\rho_g/(\pi(r + \rho_g)^2)$, $d_3 = 6L\rho_g^2/(\rho_g + \|\mathbf{x}(0) - \mathbf{x}(L)\|)^3$, and $d_4 = 8L\rho_g^2/(3\pi(\sqrt{r_1^2 + r_2^2} + \rho_g)^4)$ where ρ_g is the global radius of curvature defined in (8).

4. SIMULATION RESULTS

We select parameters that maximize the packing densities through a naive exhaustive multi-resolutional grid search and display these parameters in Table 2. In Fig. 2 we show surface plots of the computed tube packings where in the $n = 4$ case we plot the 3-D cross-section of the 4-D tube packing. Interestingly, the cross-sections of each of the n dimensional tubes tends to form sphere packings in the $n-1$ dimensional cross-sectional Euclidean space. Similar to the case with sphere packing [14], the tube packing density decreases with increasing dimension which may explain why the gap to OPTA also increases with increasing n as shown in Fig. 3. Expressing the OPTA relationship from (11) in decibels where $\text{SDR}_{dB} = 10 \log_{10}(\sigma_s^2/D)$ and $\text{SNR}_{dB} = 10 \log_{10}(P/\sigma_w^2)$

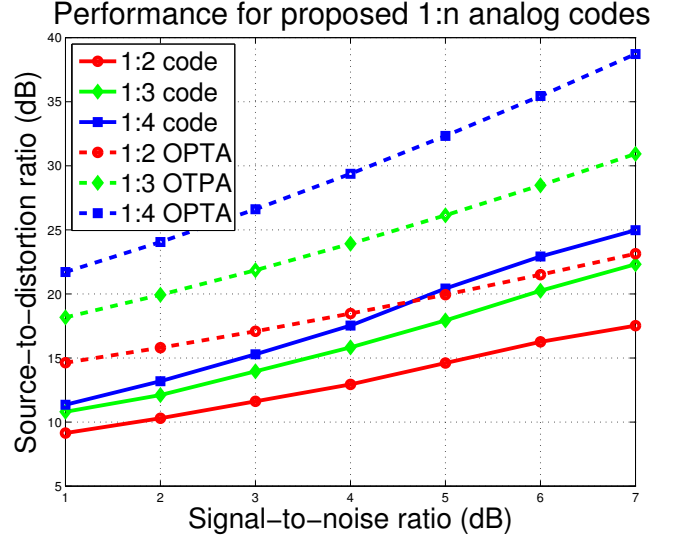


Fig. 3: SDR vs SNR of codes in Tables 1 compared to OPTA

we have

$$\text{SDR}_{dB} \leq 7.5535 + 10n \log_{10} \left(1 + 10^{\text{SNR}_{dB}/10} \right) \quad (17)$$

which is used to plot the OPTA curves against the Monte Carlo generated performance curves of our constant curvature analog codes in Fig. 3.

5. REFERENCES

- [1] C. E. Shannon, "Communication in the presence of noise," *Proc. IRE*, pp. 10–21, 1949.
- [2] V. A. Kotelnikov, *The Theory of Optimum Noise Immunity*, New York: McGraw-Hill, 1959.
- [3] M. Gastpar, B. Rimoldi, and M. Vetterli, "To code, or not to code: lossy source-channel communication revisited," *Information Theory, IEEE Transactions on*, vol. 49, no. 5, pp. 1147 – 1158, may 2003.
- [4] F. Hekland, P.A. Floor, and T.A. Ramstad, "Shannon-kotel-nikov mappings in joint source-channel coding," *Communications, IEEE Transactions on*, vol. 57, no. 1, pp. 94 –105, january 2009.
- [5] Fredrik Hekland, *On the Design and Analysis of Shannon-Kotelnikov Mappings for Joint-Source-Channel Coding*, Ph.D. thesis, NTNU, 2007.
- [6] E. Akyol, K. Rose, and T. Ramstad, "Optimal mappings for joint source channel coding," in *Information Theory Workshop (ITW), 2010 IEEE*, jan. 2010, pp. 1 –5.

- [7] A.A. Saleh, F. Alajaji, and Wai-Yip Chan, “Hybrid digital-analog source-channel coding with one-to-three bandwidth expansion,” in *Information Theory (CWIT), 2011 12th Canadian Workshop on*, may 2011, pp. 70–73.
- [8] B. Kravtsov and D. Raphaeli, “Multidimensional analog modulation and optimal mappings,” in *Global Telecommunications Conference, 2007. GLOBECOM '07. IEEE*, nov. 2007, pp. 1426–1430.
- [9] J. Ziv, “The behavior of analog communication systems,” *Information Theory, IEEE Transactions on*, vol. 16, no. 5, pp. 587–594, sep 1970.
- [10] Oscar Gonzalez, Oscar Gonzalez, John H. Maddocks, and John H. Maddocks, “Global curvature, thickness and the ideal shapes of knots,” in *Proceedings of the National Academy of Sciences, USA 96*, 1999, pp. 4769–4773.
- [11] T. Cover and J. Thomas, *Elements of Information Theory*, John Wiley and Sons, Inc., 1991.
- [12] T. Berger, *Rate Distortion Theory*, Englewood Cliffs, NJ: Prentice-Hall, 1971.
- [13] K. Nalty, “Curves of constant curvatures in four dimensional spacetime,” 2011.
- [14] J.H. Conway and N.J. Sloane, *Sphere Packing, Lattices, and Groups (Third Edition)*, Springer-Verlag, NY, 1998.
- [15] J. Smutny O. Gonzalez, J. H. Maddocks, “Curves, circles, and spheres,” *Contemporary Mathematics (AMS)*, vol. 304, pp. 195–215, 2002.
- [16] A Maritan, C Micheletti, A Trovato, and J R Banavar, “Optimal shapes of compact strings,” *Nature*, vol. 406, no. 6793, pp. 287–90, 2000.